UNIVERSIDAD DE CONCEPCIÓN

Centro de Investigación en Ingeniería Matemática (CI^{2}MA)

On the approximation of the Lamé equations considering nonhomogeneous Dirichlet boundary condition: A new approach

Tomás Barrios, Edwin Behrens,
Rommel Bustinza

PREPRINT 2024-21

SERIE DE PRE-PUBLICACIONES

On the approximation of the Lamé equations considering nonhomogeneous Dirichlet boundary condition: A new approach

Tomás P. Barrios[1,3], Edwin Behrens[2,3], and Rommel Bustinza[4,5]

[1]Departamento de Matemática y Física Aplicadas, Facultad de Ingeniería, Universidad Católica de la Santísima Concepción, Concepción, Chile
[2]Departamento de Ingeniería Civil, Facultad de Ingeniería, Universidad Católica de la Santísima Concepción, Concepción, Chile
[3]Grupo de Investigación en Análisis Numérico y Cálculo Científico, GIANuC^2, Concepción, Chile.
e-mail: tomas@ucsc.cl, ebehrens@ucsc.cl
[4]Corresponding author. Departamento de Ingeniería Matemática, Universidad de Concepción, Concepción, Chile.
e-mail: rbustinz@ing-mat.udec.cl
[5]Centro de Investigación en Ingeniería Matemática, CI^{2}MA, Concepción, Chile.

Abstract

We develop a numerical analysis for the linear elasticity problem with non homogeneous Dirichlet boundary condition, approximated by an unusual conforming finite element scheme. Specifically, for our approach, we show optimal rate of convergence for the a priori error analysis, which turns out to be valid for both 2D and 3D. In addition, we include an a posteriori error analysis based on the Ritz projection of the error, and we present an a posteriori error estimator that is reliable and local efficient. We remark that the resulting scheme has fewer degrees of freedom than many others for the same problem, that can be found in the current literature. We provide numerical experiments that illustrate the performance of the corresponding adaptive algorithm and support its use in practice.

Mathematics Subject Classifications (1991): 65N15, 65N30, 65N50, 74B05, 74S05

Key words: A posteriori error estimates, mixed finite element, augmented formulation, linear elasticity, Ritz projection

1 Introduction

This paper proposes a numerical solution for the linear elasticity problem with nonhomegeous Dirichlet boundary conditions, covering both a priori and a posteriori error analysis. In order to describe the problem of interest, we let $\Omega \subset \mathbb{R}^n$, with $n = 2, 3$, be a bounded and simply connected domain with a Lipschitz-continuous boundary $\Gamma := \partial\Omega$ of an elastic body subject to an exterior force $\boldsymbol{f} \in [L^2(\Omega)]^n$,

and a given displacement boundary condition $\boldsymbol{g}$. The kinematic model of linear elasticity seeks a displacement vector field $\tilde{\boldsymbol{u}}$ satisfying

$$\begin{cases} -\mathbf{div}(\boldsymbol{\sigma}(\tilde{\boldsymbol{u}})) = \boldsymbol{f} & \text{in} \quad \Omega\,, \\ \tilde{\boldsymbol{u}} = \boldsymbol{g} & \text{on} \quad \Gamma\,. \end{cases}$$

Hereafter, $\boldsymbol{\sigma}(\tilde{\boldsymbol{u}})$ denotes the symmetric Cauchy stress tensor, given by

$$\boldsymbol{\sigma}(\tilde{\boldsymbol{u}}) := 2\mu\,\boldsymbol{\varepsilon}(\tilde{\boldsymbol{u}}) + \lambda\,\mathrm{div}(\tilde{\boldsymbol{u}})\boldsymbol{I}\,,$$

where $\boldsymbol{\varepsilon}(\tilde{\boldsymbol{u}}) := \frac{1}{2}\left(\nabla\tilde{\boldsymbol{u}} + (\nabla\tilde{\boldsymbol{u}})^{\mathtt{t}}\right)$ represents the strain tensor, $\boldsymbol{I}$ is meant for the identity tensor of order n. In addition, μ and λ are the Lamé constants, which are given by

$$\lambda = \frac{E\nu}{(1+\nu)(1-2\nu)}, \quad \mu = \frac{E}{2(1+\nu)}\,,$$

with E being the elasticity modulus and $\nu \in (0, 1/2)$ is the Poisson's ratio.

It is very well known that the employment of dual-mixed variational formulations and the associated mixed finite element methods in linear elasticity, arrives to locking free schemes (see [7], [8] and the references therein). Probably, one of the most popular schemes is based on the mixed method of Hellinger and Reissner, providing simultaneous approximation for the stress and the displacement. In addition, at least in [2] (see also [15], [12], [13]), the symmetry of the stress tensor is imposed weakly, through the introduction of the rotation as an additional unknown.

Recently in [1], a new augmented mixed finite element method for the linear elasticity problem is developed and analysed. The authors follow the ideas previously introduced in [9], and impose the symmetry of the stress tensor weakly. This is done using a skew symmetric tensor instead of the standard strain tensor, allowing them to circumvent the use of any additional unknowns. As a consequence, the number of degrees of freedom in the discrete scheme is decreased. The nonhomogeneous boundary condition is treated by augmenting the bilinear form with an additional term of least square type, involving the Dirichlet datum. Then, the stabilization's parameters are chosen such that the resulting bilinear form results to be strongly coercive, which is usually established with the help of a Korn's type inequality.

Concerning the a posteriori error analysis for the augmented mixed formulation in linear elasticity, an a posteriori error estimator of residual type has been derived in [6], for the case of pure homogeneous Dirichlet boundary condition. Years later, in [3] the authors have extended that analysis to the case of nonhomogeneous Dirichlet and mixed boundary conditions. More recently in [4] the authors dealt with an elasticity problem with nonhomogeneous boundary conditions, deriving an a posteriori error estimator based on the Ritz projection of the error. We remark that this estimator is of low computational cost, in the sense that the estimator developed in [4] has fewer terms than those found in [3] for the same formulation of the problem. We notice that in both articles ([3] and [4]), as well as in [1], the treatment of the boundary condition is following the ideas developed in [13], that is, stabilizing the bilinear form by adding a least squares type term that involves the Dirichlet datum.

The novelty in this article is to present, for the elasticity problem with nonhomogeneous Dirichlet boundary condition, an alternative procedure for dealing with the boundary condition, to the one developed in [1]. Indeed, we first impose the symmetry of the stress tensor by using a skew symmetric

tensor instead of standard strain tensor. For the treatment of the boundary condition, we perform a homogenization procedure of the Dirichlet datum. It is important to remark that our proposal exploits the linearity of the partial differential equation in order to deal with a similar problem, having as a boundary datum a suitable polynomial approximation of the original one. From a computational point of view, this is not expensive, since the matrix of the corresponding linear system is the same. The strategy just modified the right hand side. Moreover, the corresponding a posteriori error estimator only consists of two residual terms.

The rest of the paper is organized as follows. In Section 2, we introduce the augmented variational formulation proposed for the linear elasticity problem with homogeneous Dirichlet boundary condition, the corresponding Galerkin scheme and the simplest finite element subspaces that can be used. In Section 3, we develop an a posteriori error analysis, obtaining a reliable and quasi-efficient local a posteriori error estimator. The extension of the methodology, when a nonhomogeneous Dirichlet condition for the displacement appears, is described in Section 4. Finally, in Section 5 we provide several numerical experiments that support the use of the new a posteriori error estimates in practice.

We end this section with some notations to be used throughout the paper. Given a Hilbert space H, we denote by H^n (resp., $H^{n\times n}$) the space of vectors (resp., square tensors) of order n with entries in H. Given $\boldsymbol{\tau} := (\tau_{ij})$ and $\boldsymbol{\zeta} := (\zeta_{ij}) \in \mathbb{R}^{n\times n}$, we denote $\boldsymbol{\tau}^{\mathtt{t}} := (\tau_{ji})$, $\mathrm{tr}(\boldsymbol{\tau}) := \tau_{11} + \ldots + \tau_{nn}$ and $\boldsymbol{\tau} : \boldsymbol{\zeta} := \sum_{i,j=1}^{n} \tau_{ij}\,\zeta_{ij}$. We also use the standard notations for Sobolev spaces and norms. Finally, C or c (with or without subscripts) denote generic constants, independent of the discretization parameters, that may take different values at different occurrences.

2 The augmented mixed finite element method

Since slight modifications of the analysis presented in [1], allow us to study the case with null displacement on Γ, in this section we give a brief description of the analysis, resuming the main results. These modifications are related to the fact that here the boundary datum is null, which has an impact on the fact that the spaces must be slightly redefined, and it is not necessary to augment the bilinear form with the term that involves the boundary condition.

In what follows, we denote by $\mathcal{C}$ the Hooke's law, that is,

$$\mathcal{C}\,\boldsymbol{\zeta} \;:=\; \lambda\,\mathrm{tr}(\boldsymbol{\zeta})\,\boldsymbol{I} \;+\; 2\,\mu\,\boldsymbol{\zeta}\,, \qquad \forall\,\boldsymbol{\zeta} \,\in\, [L^2(\Omega)]^{n\times n}\,,$$

It is not difficult to see that

$$\mathcal{C}^{-1}\,\boldsymbol{\zeta} \,:=\, \frac{1}{2\,\mu}\,\boldsymbol{\zeta} \,-\, \frac{\lambda}{2\,\mu\,(n\lambda+2\mu)}\,\mathrm{tr}(\boldsymbol{\zeta})\,\boldsymbol{I}\,, \qquad \forall\,\boldsymbol{\zeta} \,\in\, [L^2(\Omega)]^{n\times n}\,.$$

Next, we consider the problem: *Find the displacement $\hat{\boldsymbol{u}}$ and the stress tensor $\hat{\boldsymbol{\sigma}}$ such that*

$$\left\{\begin{array}{rcll} -\mathbf{div}(\hat{\boldsymbol{\sigma}}) &=& \boldsymbol{f} & \text{in } \Omega,\\ \mathcal{C}^{-1}\hat{\boldsymbol{\sigma}} &=& \boldsymbol{\varepsilon}(\hat{\boldsymbol{u}}) & \text{in } \Omega,\\ \hat{\boldsymbol{u}} &=& \boldsymbol{0} & \text{on } \Gamma, \end{array}\right. \tag{1}$$

The approach in [1] introduces the *skew symmetric tensor* $\boldsymbol{\gamma}(\boldsymbol{v}) := \frac{\nabla\boldsymbol{v}-(\nabla\boldsymbol{v})^{\mathtt{t}}}{2}$, for any $\boldsymbol{v} \in [H^1(\Omega)]^n$ and provides simultaneous approximations of the displacement $\hat{\boldsymbol{u}}$ and the stress tensor $\hat{\boldsymbol{\sigma}}$.

Now, we recall the well known Hilbert spaces

$$[H^1_0(\Omega)]^n := \{ \boldsymbol{v} \in [H^1(\Omega)]^n : \boldsymbol{v} = \boldsymbol{0} \quad \text{on } \Gamma \},$$

and

$$H(\mathbf{div};\Omega) := \{\boldsymbol{\tau} \in [L^2(\Omega)]^{n\times n} : \mathbf{div}(\boldsymbol{\tau}) \in [L^2(\Omega)]^n \}.$$

We set $\boldsymbol{H} := H(\mathbf{div};\Omega) \times [H^1(\Omega)]^n$, $\boldsymbol{H}_0 := H(\mathbf{div};\Omega) \times [H^1_0(\Omega)]^n$. Moreover, we endow $\boldsymbol{H}$ with the usual norm

$$\|(\boldsymbol{\tau},\boldsymbol{v})\|_{\boldsymbol{H}} := \big(\|\boldsymbol{\tau}\|^2_{H(\mathbf{div};\Omega)} + \|\boldsymbol{v}\|^2_{[H^1(\Omega)]^n}\big)^{1/2}, \quad \forall\, (\boldsymbol{\tau},\boldsymbol{v}) \in \boldsymbol{H}.$$

Next, we consider the bilinear form $A : \boldsymbol{H} \times \boldsymbol{H} \to \mathbb{R}$, given for any $(\boldsymbol{\rho},\boldsymbol{w}), (\boldsymbol{\tau},\boldsymbol{v}) \in \boldsymbol{H}$, by

$$\begin{aligned} A((\boldsymbol{\rho},\boldsymbol{w}),(\boldsymbol{\tau},\boldsymbol{v})) := & \int_\Omega \mathcal{C}^{-1}\boldsymbol{\rho} : \boldsymbol{\tau} + \int_\Omega \boldsymbol{w}\cdot\mathbf{div}(\boldsymbol{\tau}) + \int_\Omega \boldsymbol{\gamma}(\boldsymbol{w}) : \boldsymbol{\tau} - \int_\Omega \boldsymbol{v}\cdot\mathbf{div}(\boldsymbol{\rho}) - \int_\Omega \boldsymbol{\rho} : \boldsymbol{\gamma}(\boldsymbol{v}) \\ & + \kappa_1 \int_\Omega \big(\boldsymbol{\varepsilon}(\boldsymbol{w}) - \mathcal{C}^{-1}\boldsymbol{\rho}\big) : \big(\boldsymbol{\varepsilon}(\boldsymbol{v}) + \mathcal{C}^{-1}\boldsymbol{\tau}\big) + \kappa_2 \int_\Omega \mathbf{div}(\boldsymbol{\rho})\cdot\mathbf{div}(\boldsymbol{\tau}), \end{aligned} \tag{2}$$

and the linear functional $F : \boldsymbol{H} \to \mathbb{R}$ defined by

$$F(\boldsymbol{\tau},\boldsymbol{v}) := \int_\Omega \boldsymbol{f}\cdot(\boldsymbol{v} - \kappa_2\,\mathbf{div}(\boldsymbol{\tau})) \quad \forall\,(\boldsymbol{\tau},\boldsymbol{v}) \in \boldsymbol{H} \quad \forall\,(\boldsymbol{\tau},\boldsymbol{v}) \in \boldsymbol{H},$$

where κ_1 and κ_2 are positive parameters, independent of λ, at our disposal.

The augmented variational formulation proposed in [1] for problem (1), reads: Find $(\hat{\boldsymbol{\sigma}},\hat{\boldsymbol{u}}) \in \boldsymbol{H}_0$ such that

$$A((\hat{\boldsymbol{\sigma}},\hat{\boldsymbol{u}}),(\boldsymbol{\tau},\boldsymbol{v})) = F(\boldsymbol{\tau},\boldsymbol{v}), \quad \forall\,(\boldsymbol{\tau},\boldsymbol{v}) \in \boldsymbol{H}_0. \tag{3}$$

Hereafter, we assume that the stabilization parameters (κ_1,κ_2) satisfy the assumptions of Theorem 2.3 in [1]. Namely, (κ_1,κ_2) is independent of λ, $\kappa_1 \in (0, 2\,\mu)$ and $\kappa_2 > 0$ Then, there exist positive constants M and α, independent of λ, such that A is bounded in $\boldsymbol{H}$ and elliptic on $\boldsymbol{H}_0$, that is

$$|A((\hat{\boldsymbol{\sigma}},\hat{\boldsymbol{u}}),(\boldsymbol{\tau},\boldsymbol{v}))| \le M\,\|(\hat{\boldsymbol{\sigma}},\hat{\boldsymbol{u}})\|_{\boldsymbol{H}}\,\|(\boldsymbol{\tau},\boldsymbol{v})\|_{\boldsymbol{H}}, \qquad \forall\,(\hat{\boldsymbol{\sigma}},\hat{\boldsymbol{u}}),\,(\boldsymbol{\tau},\boldsymbol{v}) \in \boldsymbol{H},$$

$$A((\boldsymbol{\tau},\boldsymbol{v}),(\boldsymbol{\tau},\boldsymbol{v})) \ge \alpha\,\|(\boldsymbol{\tau},\boldsymbol{v})\|^2_{\boldsymbol{H}}, \qquad \forall\,(\boldsymbol{\tau},\boldsymbol{v}) \in \boldsymbol{H}_0.$$

As a consequence, the augmented variational formulation (3) has a unique solution $(\hat{\boldsymbol{\sigma}},\hat{\boldsymbol{u}}) \in \boldsymbol{H}_0$ and there exists a positive constant C, independent of λ, such that

$$\|(\hat{\boldsymbol{\sigma}},\hat{\boldsymbol{u}})\|_{\boldsymbol{H}} \le C\,\|\boldsymbol{f}\|_{[L^2(\Omega)]^n}.$$

Now, let h be a positive parameter and consider finite dimensional subspace $\boldsymbol{H}_{0,h} \subset \boldsymbol{H}_0$. Then, the Galerkin scheme associated to problem (3), reads: Find $(\hat{\boldsymbol{\sigma}}_h,\hat{\boldsymbol{u}}_h) \in \boldsymbol{H}_{0,h}$ such that

$$A((\hat{\boldsymbol{\sigma}}_h,\hat{\boldsymbol{u}}_h),(\boldsymbol{\tau}_h,\boldsymbol{v}_h)) = F(\boldsymbol{\tau}_h,\boldsymbol{v}_h) \quad \forall\,(\boldsymbol{\tau}_h,\boldsymbol{v}_h) \in \boldsymbol{H}_{0,h}. \tag{4}$$

The well posedness of problem (4) needs to be proved for any choice of the finite element subspaces $\boldsymbol{H}_{0,h} \subset \boldsymbol{H}_0$. Next we describe the simplest choice of $\boldsymbol{H}_{0,h}$ that preserves stability. In what follows, we assume that Ω is a polygonal/polyhedral region and let $\{\mathcal{T}_h\}_{h>0}$ be a regular family of triangulations of $\bar{\Omega}$ made of simplicial cells, such that $\bar{\Omega} = \cup\{T : T \in \mathcal{T}_h\}$. Given an element $T \in \mathcal{T}_h$, we denote

by h_T its diameter and define the mesh size $h := \max\{ h_T : T \in \mathcal{T}_h \}$. In addition, given an integer $\ell \geq 0$ and a subset S of $\mathbb{R}^n$, we denote by $\P_\ell(S)$ the space of polynomials in n variables defined in S of total degree at most ℓ. Moreover, for each $T \in \mathcal{T}_h$, we define the local Raviart-Thomas space of order ℓ, $\mathcal{RT}_\ell(T) := [\P_\ell(T)]^n \oplus \P_\ell(T)\,\boldsymbol{x} \subseteq [\P_{\ell+1}(T)]^n$, where $\boldsymbol{x} := (x_1, \ldots, x_n)^{\mathtt{t}}$ is a generic vector of $\mathbb{R}^n$. Then, we define the finite element subspaces

$$H_h^{\boldsymbol{\sigma}} := \left\{ \boldsymbol{\tau}_h \in H(\mathbf{div};\Omega) : \boldsymbol{\tau}_h|_T \in [\mathcal{RT}_0(T)^{\mathtt{t}}]^n, \quad \forall\, T \in \mathcal{T}_h \right\},$$

$$H_h^{\boldsymbol{u}} := \left\{ \boldsymbol{v}_h \in [\mathcal{C}(\bar{\Omega})]^n : \boldsymbol{v}_h|_T \in [\P_1(T)]^n, \quad \forall\, T \in \mathcal{T}_h \right\},$$

$$H_{0,h}^{\boldsymbol{u}} := \{ \boldsymbol{v}_h \in H_h^{\boldsymbol{u}} : \boldsymbol{v}_h = \mathbf{0} \quad \text{on } \Gamma \}\,.$$

Then, the simplest choice of stable finite element subspaces (cf. [12]) is given by

$$\boldsymbol{H}_{0,h} := H_h^{\boldsymbol{\sigma}} \times H_{0,h}^{\boldsymbol{u}} \subseteq \boldsymbol{H}_0\,.$$

The following result allows us to recall the rate of convergence of the Galerkin scheme (4) for this particular choice of finite element subspaces.

Theorem 1 *Let $(\hat{\boldsymbol{\sigma}}, \hat{\boldsymbol{u}}) \in \boldsymbol{H}_0$ and $(\hat{\boldsymbol{\sigma}}_h, \hat{\boldsymbol{u}}_h) \in \boldsymbol{H}_{0,h}$ be the unique solutions to problems (3) and (4), respectively. In addition, assume that $\boldsymbol{\sigma} \in [H^r(\Omega)]^{n\times n}$, $\mathbf{div}(\boldsymbol{\sigma}) \in [H^r(\Omega)]^n$, $\boldsymbol{u} \in [H^{r+1}(\Omega)]^n$, for some $r \in (0,1]$. Then, there exists $C > 0$, independent of λ, h, such that there holds*

$$\|(\hat{\boldsymbol{\sigma}}, \hat{\boldsymbol{u}},) - (\hat{\boldsymbol{\sigma}}_h, \hat{\boldsymbol{u}}_h)\|_{\boldsymbol{H}} \leq C\, h^r \left(\|\hat{\boldsymbol{\sigma}}\|_{[H^r(\Omega)]^{n\times n}} + \|\mathbf{div}(\hat{\boldsymbol{\sigma}})\|_{[H^r(\Omega)]^n} + \|\hat{\boldsymbol{u}}\|_{[H^{r+1}(\Omega)]^n} \right).$$

Proof. It is a consequence of the coercivity of A, Céa's estimate and the corresponding approximation properties of the finite element spaces. We refer to Section 3.3 in [1], for further details. □

3 A posteriori error analysis

In this section, we follow the ideas given in [4], and develop an a posteriori error analysis for the discrete scheme (4), using an appropriate Ritz projection of the error. First, we introduce the usual inner product of $\boldsymbol{H}$

$$\langle (\boldsymbol{\rho}, \boldsymbol{w}), (\boldsymbol{\tau}, \boldsymbol{v}) \rangle_{\boldsymbol{H}} := (\boldsymbol{\rho}, \boldsymbol{\tau})_{H(\mathbf{div};\Omega)} + (\boldsymbol{w}, \boldsymbol{v})_{[H^1(\Omega)]^n} \quad \forall\, (\boldsymbol{\rho}, \boldsymbol{w}), (\boldsymbol{\tau}, \boldsymbol{v}) \in \boldsymbol{H}\,,$$

and let $(\hat{\boldsymbol{\sigma}}, \hat{\boldsymbol{u}})$ and $(\hat{\boldsymbol{\sigma}}_h, \hat{\boldsymbol{u}}_h)$ be the unique solutions to problem (3) and (4), respectively. We define the Ritz projection of the error with respect to the as the unique element $(\bar{\boldsymbol{\sigma}}, \bar{\boldsymbol{u}}) \in \boldsymbol{H}_0$ such that

$$\langle (\bar{\boldsymbol{\sigma}}, \bar{\boldsymbol{u}}), (\boldsymbol{\tau}, \boldsymbol{v}) \rangle_{\boldsymbol{H}} = A((\hat{\boldsymbol{\sigma}} - \hat{\boldsymbol{\sigma}}_h, \hat{\boldsymbol{u}} - \hat{\boldsymbol{u}}_h), (\boldsymbol{\tau}, \boldsymbol{v})) \quad \forall\, (\boldsymbol{\tau}, \boldsymbol{v}) \in \boldsymbol{H}_0\,. \tag{5}$$

We remark that the existence and uniqueness of $(\bar{\boldsymbol{\sigma}}, \bar{\boldsymbol{u}}) \in \boldsymbol{H}_0$ is guaranteed by the Riesz' representation theorem.

On the other hand, using the continuous dependence of the solution on the data, we are able to bound the error in terms of its Ritz projection, as follows:

$$||(\hat{\boldsymbol{\sigma}} - \hat{\boldsymbol{\sigma}}_h, \hat{\boldsymbol{u}} - \hat{\boldsymbol{u}}_h)||_{\boldsymbol{H}} \leq C\, ||(\bar{\boldsymbol{\sigma}}, \bar{\boldsymbol{u}})||_{\boldsymbol{H}}\,. \tag{6}$$

Then, according to (6), in order to obtain reliable a posteriori error estimates for the discrete scheme (4), it is enough to bound from above the Ritz projection of the error. In the next lemma we obtain an upper bound for $||(\bar{\boldsymbol{\sigma}}, \bar{\boldsymbol{u}})||_{\boldsymbol{H}}$ in terms of residuals.

Lemma 2 *There exists a constant $C > 0$, independent of λ and h, such that*

$$||(\bar{\boldsymbol{\sigma}}, \bar{\boldsymbol{u}})||_{\boldsymbol{H}} \leq C \left(||\boldsymbol{f} + \mathbf{div}(\hat{\boldsymbol{\sigma}}_h)||_{[L^2(\Omega)]^n} + ||\boldsymbol{\varepsilon}(\hat{\boldsymbol{u}}_h) - \mathcal{C}^{-1}\hat{\boldsymbol{\sigma}}_h||_{[L^2(\Omega)]^{n\times n}} \right). \tag{7}$$

Proof. We first use the fact that $(\hat{\boldsymbol{\sigma}}, \hat{\boldsymbol{u}}) \in \boldsymbol{H}_0$ is the unique solution to problem (3), to obtain

$$\langle (\bar{\boldsymbol{\sigma}}, \bar{\boldsymbol{u}}), (\boldsymbol{\tau}, \boldsymbol{v}) \rangle_{\boldsymbol{H}} = F(\boldsymbol{\tau}, \boldsymbol{v}) - A((\hat{\boldsymbol{\sigma}}_h, \hat{\boldsymbol{u}}_h), (\boldsymbol{\tau}, \boldsymbol{v})), \quad \forall\, (\boldsymbol{\tau}, \boldsymbol{v}) \in \boldsymbol{H}_0 .$$

The latter is equivalently to

$$\begin{cases} (\bar{\boldsymbol{\sigma}}, \boldsymbol{\tau})_{H(\mathbf{div};\Omega)} = R_1(\boldsymbol{\tau}), & \forall\, \boldsymbol{\tau} \in H(\mathbf{div};\Omega), \\ (\bar{\boldsymbol{u}}, \boldsymbol{v})_{[H^1(\Omega)]^n} = R_2(\boldsymbol{v}), & \forall\, \boldsymbol{v} \in [H_0^1(\Omega)]^n, \end{cases}$$

where $R_1 : H(\mathbf{div};\Omega) \to \mathbb{R}$ and $R_2 : [H_0^1(\Omega)]^n \to \mathbb{R}$ are the bounded linear functionals, defined by

$$\begin{aligned} R_1(\boldsymbol{\tau}) := & -\kappa_2 \int_\Omega (\boldsymbol{f} + \mathbf{div}(\hat{\boldsymbol{\sigma}}_h)) \cdot \mathbf{div}(\boldsymbol{\tau}) - \int_\Omega (\mathcal{C}^{-1}\hat{\boldsymbol{\sigma}}_h - \boldsymbol{\varepsilon}(\hat{\boldsymbol{u}}_h)) : \boldsymbol{\tau} \\ & - \kappa_1 \int_\Omega (\boldsymbol{\varepsilon}(\hat{\boldsymbol{u}}_h) - \mathcal{C}^{-1}\hat{\boldsymbol{\sigma}}_h) : \mathcal{C}^{-1}\boldsymbol{\tau}, \quad \forall\, \boldsymbol{\tau} \in H(\mathbf{div};\Omega) \\ R_2(\boldsymbol{v}) := & \int_\Omega (\boldsymbol{f} + \mathbf{div}(\hat{\boldsymbol{\sigma}}_h)) \cdot \boldsymbol{v} - \kappa_1 \int_\Omega \left(\boldsymbol{\varepsilon}(\hat{\boldsymbol{u}}_h) - \mathcal{C}^{-1}\hat{\boldsymbol{\sigma}}_h\right) : \boldsymbol{\varepsilon}(\boldsymbol{v}), \quad \forall\, \boldsymbol{v} \in [H_0^1(\Omega)]^n . \end{aligned}$$

Then, the result follows after applying the Cauchy-Schwarz inequality, the continuity of $\mathcal{C}^{-1}$ and the definition of the $\boldsymbol{H}$-norm. □ Lemma 2 leads us to define the following a posteriori error estimator

$$\hat{\eta} := \left(\sum_{T \in \mathcal{T}_h} \hat{\eta}_T^2 \right)^{1/2},$$

where

$$\forall\, T \in \mathcal{T} : \hat{\eta}_T^2 := ||\boldsymbol{f} + \mathbf{div}(\hat{\boldsymbol{\sigma}}_h)||^2_{[L^2(T)]^n} + ||\boldsymbol{\varepsilon}(\hat{\boldsymbol{u}}_h) - \mathcal{C}^{-1}\hat{\boldsymbol{\sigma}}_h||^2_{[L^2(T)]^{n\times n}} .$$

In the next result, we establish that the a posteriori error estimator $\hat{\eta}$ is reliable and efficient.

Theorem 3 *There exist positive constants, $C_{\mathtt{eff}}$ and $C_{\mathtt{rel}}$, independent of h and λ, such that*

$$C_{\mathtt{eff}}\, \hat{\eta} \leq ||((\hat{\boldsymbol{\sigma}} - \hat{\boldsymbol{\sigma}}_h, \hat{\boldsymbol{u}} - \hat{\boldsymbol{u}}_h)||_{\boldsymbol{H}} \leq C_{\mathtt{rel}}\, \hat{\eta}. \tag{8}$$

Proof. The reliability of $\hat{\eta}$ (inequality on the right hand side of (8)) follows from its definition and (6)–(7). To prove that $\hat{\eta}$ is efficient (inequality on the left hand side of (8)), we proceed similarly as in [6]. In this way, noticing that $\boldsymbol{f} = -\mathbf{div}(\hat{\boldsymbol{\sigma}})$ and $\boldsymbol{\varepsilon}(\hat{\boldsymbol{u}}) = \mathcal{C}^{-1}\hat{\boldsymbol{\sigma}}$ in Ω, we have

$$\begin{aligned} ||\boldsymbol{f} + \mathbf{div}(\hat{\boldsymbol{\sigma}}_h)||_{[L^2(T)]^n} &= ||\mathbf{div}(\hat{\boldsymbol{\sigma}}_h - \hat{\boldsymbol{\sigma}})||_{[L^2(T)]^n}, \\ ||\boldsymbol{\varepsilon}(\hat{\boldsymbol{u}}_h) - \mathcal{C}^{-1}\hat{\boldsymbol{\sigma}}_h||_{[L^2(T)]^{n\times n}} &\leq ||\boldsymbol{\varepsilon}(\hat{\boldsymbol{u}}_h) - \boldsymbol{\varepsilon}(\hat{\boldsymbol{u}})||_{[L^2(T)]^{n\times n}} + ||\mathcal{C}^{-1}(\hat{\boldsymbol{\sigma}} - \hat{\boldsymbol{\sigma}}_h)||_{[L^2(T)]^{n\times n}} \\ &\leq \left(||\hat{\boldsymbol{u}} - \hat{\boldsymbol{u}}_h||_{[H^1(T)]^n} + \frac{1}{\mu}(||\hat{\boldsymbol{\sigma}} - \hat{\boldsymbol{\sigma}}_h||_{[L^2(T)]^{n\times n}} \right) \\ &\leq \max\{1, 1/\mu\} \left(||\hat{\boldsymbol{u}} - \hat{\boldsymbol{u}}_h||_{[H^1(T)]^n} + ||\hat{\boldsymbol{\sigma}} - \hat{\boldsymbol{\sigma}}_h||_{[L^2(T)]^{n\times n}} \right). \end{aligned}$$

□

4 Nonhomogeneous Dirichlet boundary condition

We remark that the novelty of the current work, relies on the treatment of nonhomogeneous Dirichlet boundary condition, which will be described in this section. To this aim, given the data $\boldsymbol{f} \in [L^2(\Omega)]^n$ and $\boldsymbol{g} \in [H^{1/2}(\Gamma)]^n$, we consider the problem: *Find the displacement field* $\tilde{\boldsymbol{u}} \in [H^1(\Omega)]^n$ *such that*

$$\begin{cases} -\mathbf{div}(\boldsymbol{\sigma}(\tilde{\boldsymbol{u}})) = \boldsymbol{f} & \text{in} \quad \Omega\,, \\ \tilde{\boldsymbol{u}} = \boldsymbol{g} & \text{on} \quad \Gamma\,, \end{cases}$$

where, as described in Section 1, $\boldsymbol{\sigma}(\tilde{\boldsymbol{u}})$ represents the Cauchy stress tensor.

Now, introducing the stress, $\tilde{\boldsymbol{\rho}} := \boldsymbol{\sigma}(\tilde{\boldsymbol{u}})$ as a new unknown, we arrive to the following first order system: Find $\tilde{\boldsymbol{\rho}} \in H(\mathbf{div};\Omega)$ and $\tilde{\boldsymbol{u}} \in [H^1(\Omega)]^n$ such that

$$\begin{cases} \mathcal{C}^{-1}\tilde{\boldsymbol{\rho}} = \boldsymbol{\varepsilon}(\tilde{\boldsymbol{u}}) & \text{in} \quad \Omega\,, \\ -\mathbf{div}(\tilde{\boldsymbol{\rho}}) \,=\, \boldsymbol{f} & \text{in} \quad \Omega\,, \\ \tilde{\boldsymbol{u}} = \boldsymbol{g} & \text{on} \quad \Gamma\,, \end{cases} \tag{9}$$

Now, we denote by $\boldsymbol{w} \in [H^1(\Omega)]^n$ the unique weak solution of the auxiliary problem:

$$-\Delta \boldsymbol{w} \,=\, 0 \quad \text{in} \quad \Omega\,, \quad \boldsymbol{w} \,=\, \boldsymbol{g} \quad \text{on} \quad \Gamma\,. \tag{10}$$

We emphasize that it is well known that $\boldsymbol{w}$ satisfies the following stability condition: There exists $C_1 > 0$, such that $||\boldsymbol{w}||_{[H^1(\Omega)]^n} \leq C_1\, ||\boldsymbol{g}||_{[H^{1/2}(\Gamma)]^n}$. Decomposing the displacement $\tilde{\boldsymbol{u}} := \hat{\boldsymbol{u}} + \boldsymbol{w}$, the first order system (9) can be rewritten as follows: *Find* $(\tilde{\boldsymbol{\rho}}, \hat{\boldsymbol{u}}) \in \boldsymbol{H}_0$ *such that*

$$\begin{cases} \mathcal{C}^{-1}\tilde{\boldsymbol{\rho}} \,-\, \boldsymbol{\varepsilon}(\hat{\boldsymbol{u}}) \,=\, \boldsymbol{\varepsilon}(\boldsymbol{w}) & \text{in} \quad \Omega\,, \\ -\mathbf{div}(\tilde{\boldsymbol{\rho}}) \,=\, \boldsymbol{f} & \text{in} \quad \Omega\,, \\ \hat{\boldsymbol{u}} \,=\, \mathbf{0} & \text{on} \quad \Gamma\,, \end{cases} \tag{11}$$

where $\boldsymbol{H}_0 := H(\mathbf{div};\Omega) \times [H^1_0(\Omega)]^n$ is the same space introduced in Section 2. Comparing (1) and (11), we notice that the only difference between them relies on the presence of term $\boldsymbol{\varepsilon}(\boldsymbol{w})$ on the right hand side of the first equation in (11). Despite this, the approach that we present here for the treatment of the inhomogeneous boundary condition, differs from the one introduced in [1]. Therefore, in what follows, we describe the deduction of the stabilized variational formulation.

Now, proceeding as in [9], we have $\boldsymbol{\varepsilon}(\hat{\boldsymbol{u}}) \,=\, \nabla \hat{\boldsymbol{u}} - \boldsymbol{\gamma}(\hat{\boldsymbol{u}})$ in Ω. This allows us to rewrite the first equation in (11) as

$$\mathcal{C}^{-1}\tilde{\boldsymbol{\rho}} \,-\, \nabla \hat{\boldsymbol{u}} \,+\, \boldsymbol{\gamma}(\hat{\boldsymbol{u}}) \,=\, \boldsymbol{\varepsilon}(\boldsymbol{w}) \quad \text{in} \quad \Omega\,, \tag{12}$$

while the symmetry of the Cauchy stress tensor implies that

$$\int_\Omega \boldsymbol{\gamma}(\boldsymbol{v}) \,:\, \tilde{\boldsymbol{\rho}} \,=\, 0 \quad \text{in} \quad \Omega \quad \forall\, \boldsymbol{v} \in [H^1_0(\Omega)]^n\,, \tag{13}$$

These equations allow us to introduce the following mixed variational formulation: *Find* $(\tilde{\boldsymbol{\rho}}, \hat{\boldsymbol{u}}) \in \boldsymbol{H}_0$ *such that*

$$\int_\Omega \mathcal{C}^{-1}\tilde{\boldsymbol{\rho}} : \boldsymbol{\tau} + \int_\Omega \hat{\boldsymbol{u}} \cdot \mathbf{div}(\boldsymbol{\tau}) + \int_\Omega \boldsymbol{\gamma}(\hat{\boldsymbol{u}}) : \boldsymbol{\tau} = \int_\Omega \boldsymbol{\varepsilon}(\boldsymbol{w}) : \boldsymbol{\tau} \qquad \forall\, \boldsymbol{\tau} \in H(\mathbf{div};\Omega)\,, \tag{14}$$

$$-\int_\Omega \boldsymbol{v} \cdot \mathbf{div}(\tilde{\boldsymbol{\rho}}) - \int_\Omega \boldsymbol{\gamma}(\boldsymbol{v}) : \tilde{\boldsymbol{\rho}} = \int_\Omega \boldsymbol{f} \cdot \boldsymbol{v} \qquad \forall\, \boldsymbol{v} \in [H_0^1(\Omega)]^n. \tag{15}$$

Now, considering κ_1 and κ_2 positive parameters, independent of λ, nd at our disposal, we include the least squares terms given by

$$\kappa_1 \int_\Omega \Big(\boldsymbol{\varepsilon}(\hat{\boldsymbol{u}}) - \mathcal{C}^{-1}\tilde{\boldsymbol{\rho}}\Big) : \Big(\boldsymbol{\varepsilon}(\boldsymbol{v}) + \mathcal{C}^{-1}\boldsymbol{\tau}\Big) = -\kappa_1 \int_\Omega \boldsymbol{\varepsilon}(\boldsymbol{w}) : \Big(\boldsymbol{\varepsilon}(\boldsymbol{v}) + \mathcal{C}^{-1}\boldsymbol{\tau}\Big) \qquad \forall\, (\boldsymbol{\tau}, \boldsymbol{v}) \in \boldsymbol{H}_0\,, \tag{16}$$

$$\kappa_2 \int_\Omega \mathbf{div}\tilde{\boldsymbol{\rho}}) \cdot \mathbf{div}(\boldsymbol{\tau}) = -\kappa_2 \int_\Omega \boldsymbol{f} \cdot \mathbf{div}(\boldsymbol{\tau}) \qquad \forall \boldsymbol{\tau} \in H(\mathbf{div};\Omega)\,. \tag{17}$$

Then adding (14), (15), (16) and (17), we obtain the following variational formulation: *Find* $(\tilde{\boldsymbol{\rho}}, \hat{\boldsymbol{u}}) \in \boldsymbol{H}_0$ *such that*

$$A((\tilde{\boldsymbol{\rho}}, \hat{\boldsymbol{u}}), (\boldsymbol{\tau}, \boldsymbol{v})) = \tilde{F}(\boldsymbol{\tau}, \boldsymbol{v})\,, \qquad \forall\, (\boldsymbol{\tau}, \boldsymbol{v}) \in \boldsymbol{H}_0\,, \tag{18}$$

where the bilinear form $A : \boldsymbol{H} \times \boldsymbol{H} \to \mathbb{R}$ has been introduced in (2), while the linear functional $\tilde{F} : \boldsymbol{H} \to \mathbb{R}$ is defined by

$$\tilde{F}(\boldsymbol{\tau}, \boldsymbol{v}) := \int_\Omega \boldsymbol{\varepsilon}(\boldsymbol{w}) : \boldsymbol{\tau} - \kappa_1 \int_\Omega \boldsymbol{\varepsilon}(\boldsymbol{w}) : (\boldsymbol{\varepsilon}(\boldsymbol{v}) + \mathcal{C}^{-1}\boldsymbol{\tau}) + \int_\Omega \boldsymbol{f} \cdot (\boldsymbol{v} - \kappa_2\, \mathbf{div}(\boldsymbol{\tau})) \quad \forall\, (\boldsymbol{\tau}, \boldsymbol{v}) \in \boldsymbol{H}\,.$$

Straightforward application of Cauchy-Schwarz inequality and the stability condition of $\boldsymbol{w}$ with respect to the datum $\boldsymbol{g}$, implies that $\tilde{F}$ is bounded, that is, there exists a constant $C^* > 0$, such that $||\tilde{F}||_{\boldsymbol{H}'} \leq C^*(\|\boldsymbol{f}\|_{[L^2(\Omega)]^n} + \|\boldsymbol{g}\|_{[H^{1/2}(\Gamma)]^n})$. Additionally, in view of what has been developed in Section 2 regarding the bilinear form A, and under the same assumptions on the parameters (κ_1, κ_2), we conclude that the problem (18) has one and only one solution, thanks to the Lax-Milgram Theorem. As a consequence, we obtain that there exists $c > 0$, such that,

$$\|(\tilde{\boldsymbol{\rho}}, \hat{\boldsymbol{u}})\|_{\boldsymbol{H}} \leq c \left(\|\boldsymbol{f}\|_{[L^2(\Omega)]^n} + \|\boldsymbol{g}\|_{[H^{1/2}(\Gamma)]^n}\right).$$

In addition, the above inequality allows us to deduce the continuous dependence on the data, of the solution of the problem (9). This means that there exists a constant $\bar{C} > 0$, such that

$$\|(\tilde{\boldsymbol{\rho}}, \boldsymbol{u})\|_{\boldsymbol{H}} = \|(\tilde{\boldsymbol{\rho}}, \hat{\boldsymbol{u}}) + (0, \boldsymbol{w})\|_{\boldsymbol{H}} \leq \bar{C} \left(\|\boldsymbol{f}\|_{[L^2(\Omega)]^n} + \|\boldsymbol{g}\|_{[H^{1/2}(\Gamma)]^n}\right). \tag{19}$$

Remark 4 *In order to solve problem* (18)*, one can think of approximating the solution of the auxiliary problem* (10)*. Unfortunately, this could carry into a high computational cost. In the next section we provide an alternative procedure.*

4.1 A priori error analysis

From now on, we assume that the parameters κ_1 and κ_2, part of the definitions of bilinear form A (cf. (2)) and $\tilde{F}$, satisfy the same conditions given in Section 2: $\kappa_1 \in (0, \mu)$ and $\kappa_2 > 0$. In this way, we ensure existence and uniqueness of discrete solution for any subspace of finite elements given. In particular, for those subspaces considered in Section 2. Indeed, we denote by $\boldsymbol{H}_{0,h} := H_h^{\boldsymbol{\sigma}} \times H_{0,h}^{\boldsymbol{u}}$, where $H_h^{\boldsymbol{\sigma}}$ and $H_{0,h}^{\boldsymbol{u}}$ are the same discrete spaces defined in Section 2.

In what follows, we denote by $E(\Gamma)$ the list of all edges/faces induced by the triangulation $\mathcal{T}_h$ on the boundary Γ. Next, we set $\boldsymbol{g}_h := \pi_h^1 \boldsymbol{g}$ on $E(\Gamma)$, with $\pi_h^1 \boldsymbol{g}$ the orthogonal L^2-projection of the function $\boldsymbol{g}$ onto $P_1(E(\Gamma))$, component-wise, i.e. $\boldsymbol{g}_h|_e \in [\mathcal{P}_1(e)]^n$ for all $e \in E(\Gamma)$. Now, we define $\boldsymbol{w}_h$ as the piecewise linear continuous function such that $\boldsymbol{w}_h(\boldsymbol{x}) = \boldsymbol{0}$ for each node $\boldsymbol{x} \in \Omega$ and $\boldsymbol{w}_h = \boldsymbol{g}_h$ on Γ. Clearly, $\boldsymbol{w}_h \in [H^1(\Omega)]^n$ and, in the sense of distributions, $-\mathbf{div}(\nabla(\boldsymbol{w}_h)) = 0$ in Ω. This leads us to the following equations

$$-\Delta(\boldsymbol{w} - \boldsymbol{w}_h) \,=\, 0 \quad \text{in} \quad \Omega\,, \qquad \boldsymbol{w} - \boldsymbol{w}_h \,=\, \boldsymbol{g} - \boldsymbol{g}_h \quad \text{on} \quad \Gamma\,. \tag{20}$$

Therefore, the stability of the solution with respect to the data, implies that there exists $C > 0$, such that

$$\|\boldsymbol{w} - \boldsymbol{w}_h\|_{[H^1(\Omega)]^n} \leq C \|\boldsymbol{g} - \boldsymbol{g}_h\|_{[H^{1/2}(\Gamma)]^n}\,. \tag{21}$$

Next, to approximate the solution of problem (9), we consider the problem: *Find* $(\bar{\boldsymbol{\rho}}, \bar{\boldsymbol{u}}) \in \boldsymbol{H}$*, such that*

$$\begin{cases} \mathcal{C}^{-1}\bar{\boldsymbol{\rho}} - \nabla \bar{\boldsymbol{u}} + \boldsymbol{\gamma}(\bar{\boldsymbol{u}}) \,=\, \boldsymbol{0} & \text{in} \quad \Omega\,, \\ -\mathbf{div}(\bar{\boldsymbol{\rho}}) \,=\, \boldsymbol{f} & \text{in} \quad \Omega\,, \\ \bar{\boldsymbol{u}} = \boldsymbol{g}_h & \text{on} \quad \Gamma\,. \end{cases} \tag{22}$$

Hence, we decompose $\bar{\boldsymbol{u}} = \boldsymbol{u} + \boldsymbol{w}_h$, and the first order system (22) is rewritten in terms of $(\bar{\boldsymbol{\rho}}, \boldsymbol{u}) \in \boldsymbol{H}_0$ as

$$\begin{cases} \mathcal{C}^{-1}\bar{\boldsymbol{\rho}} - \nabla \boldsymbol{u} + \boldsymbol{\gamma}(\boldsymbol{u}) \,=\, \boldsymbol{\varepsilon}(\boldsymbol{w}_h) & \text{in} \quad \Omega\,, \\ -\mathbf{div}(\bar{\boldsymbol{\rho}}) \,=\, \boldsymbol{f} & \text{in} \quad \Omega\,, \\ \boldsymbol{u} \,=\, \boldsymbol{0} & \text{on} \quad \Gamma\,, \end{cases} \tag{23}$$

Thus, the discrete variational formulation to approximate problem (23) consists in: *Find* $(\bar{\boldsymbol{\rho}}_h, \boldsymbol{u}_h) \in \boldsymbol{H}_{0,h}$ *such that*

$$A((\bar{\boldsymbol{\rho}}_h, \boldsymbol{u}_h), (\boldsymbol{\tau}_h, \boldsymbol{v}_h)) = \bar{F}(\boldsymbol{\tau}_h, \boldsymbol{v}_h)\,, \qquad \forall\, (\boldsymbol{\tau}_h, \boldsymbol{v}_h) \in \boldsymbol{H}_{0,h}, \tag{24}$$

where the functional $\bar{F}$ is obtained simply by replacing $\boldsymbol{w}_h$ instead of $\boldsymbol{w}$, in the definition of $\tilde{F}$.

We remark that, under the same assumption on the parameters κ_1 and κ_2, the Galerkin scheme (24) is well posed and a Céa's estimate can be obtained. In addition, the corresponding rate of convergence of the Galerkin scheme (24) for this particular choice of finite element subspaces, is presented in the next theorem. Previously, given $s > 0$, we introduce the notation for the broken spaces $H^s(\mathcal{T}_h) := \Pi_{T \in \mathcal{T}_h} H^s(T)$. Analogously, we introduce the vectorial broken spaces $[H^s(\mathcal{T}_h)]^n$.

Theorem 5 *Let $(\bar{\boldsymbol{\rho}}, \boldsymbol{u}) \in \boldsymbol{H}_0$ and $(\bar{\boldsymbol{\rho}}_h, \boldsymbol{u}_h) \in \boldsymbol{H}_{0,h}$ be the unique solutions of problems* (23) *and* (24)*, respectively. In addition, assume that $\bar{\boldsymbol{\rho}} \in [H^t(\mathcal{T}_h)]^{n\times n}$, $\mathbf{div}(\bar{\boldsymbol{\rho}}) \in [H^t(\mathcal{T}_h)]^n$ and $\boldsymbol{u} \in [H^{t+1}(\mathcal{T}_h)]^n$ for some $t \in (0, m+1]$. Then, there exists $\bar{C}_* > 0$, independent of h, such that there holds*

$$\|(\bar{\boldsymbol{\rho}}, \boldsymbol{u}) - (\bar{\boldsymbol{\rho}}_h, \boldsymbol{u}_h)\|^2_{\boldsymbol{H}} \leq \bar{C}_* \sum_{T\in\mathcal{T}_h} h_T^{2\min(t,r+1,m)} \left(\|\bar{\boldsymbol{\rho}}\|^2_{[H^t(T)]^n} + \|\mathbf{div}(\bar{\boldsymbol{\rho}})\|^2_{[H^t(T)]^n} + \|\boldsymbol{u}\|^2_{[H^{1+t}(T)]^n} \right).$$

Proof. Thanks to the ellipticity of the bilinear form A in $\boldsymbol{H}_0$, there exists a constant $C_{\mathtt{Cea}} > 0$, independent of h, such that

$$||(\bar{\boldsymbol{\rho}} - \bar{\boldsymbol{\rho}}_h, \boldsymbol{u} - \boldsymbol{u}_h)||_{\boldsymbol{H}} \leq C_{\mathtt{Cea}} \inf_{(\boldsymbol{\tau}_h, \boldsymbol{v}_h)\in\boldsymbol{H}_{0,h}} ||(\bar{\boldsymbol{\rho}} - \boldsymbol{\tau}_h, \boldsymbol{u} - \boldsymbol{v}_h)||_{\boldsymbol{H}}.$$

The rest relies on bounding the infimum by taking $(\boldsymbol{\tau}_h, \boldsymbol{v}_h) := (\pi_h^{\mathtt{RT}}(\bar{\boldsymbol{\rho}}), \pi_h^k(\boldsymbol{u}))$, the standard orthogonal projection of $\bar{\boldsymbol{\rho}}$ and $\boldsymbol{u}$ onto $H_h^{\boldsymbol{\sigma}}$ and $H_{0,h}^{\boldsymbol{u}}$, respectively. The proof follows after invoking very well known approximation properties of these projectors. We omit further details. □

Now, we introduce $\bar{\boldsymbol{u}}_h := \boldsymbol{u}_h + \boldsymbol{w}_h$. As a first consequence, we notice that

$$||(\bar{\boldsymbol{\rho}} - \bar{\boldsymbol{\rho}}_h, \bar{\boldsymbol{u}} - \bar{\boldsymbol{u}}_h)||_{\boldsymbol{H}} = ||(\bar{\boldsymbol{\rho}} - \bar{\boldsymbol{\rho}}_h, \boldsymbol{u} - \boldsymbol{u}_h)||_{\boldsymbol{H}},$$

that is, the approximation of the solution of the problem (22) by the pair $(\bar{\boldsymbol{\rho}}_h, \bar{\boldsymbol{u}}_h)$, has the same convergence rate than the problem (23), given in Theorem 5.

Furthermore, after applying triangle inequality, we obtain

$$||(\tilde{\boldsymbol{\rho}} - \bar{\boldsymbol{\rho}}_h, \tilde{\boldsymbol{u}} - \bar{\boldsymbol{u}}_h)||_{\boldsymbol{H}} \leq ||(\tilde{\boldsymbol{\rho}} - \bar{\boldsymbol{\rho}}, \tilde{\boldsymbol{u}} - \bar{\boldsymbol{u}})||_{\boldsymbol{H}} + ||(\bar{\boldsymbol{\rho}} - \bar{\boldsymbol{\rho}}_h, \bar{\boldsymbol{u}} - \bar{\boldsymbol{u}}_h)||_{\boldsymbol{H}}.$$

This means that the error of approximating the solution of the problem (9) by the pair $(\bar{\boldsymbol{\rho}}_h, \bar{\boldsymbol{u}}_h)$, is controlled by the error that is committed when approximating the Dirichlet datum, plus the error associated with the finite element method given in Theorem 5.

On the other hand, the pair $(\tilde{\boldsymbol{\rho}} - \bar{\boldsymbol{\rho}}, \tilde{\boldsymbol{u}} - \bar{\boldsymbol{u}}) \in \boldsymbol{H}_0$ satisfies, in weak sense,

$$\begin{cases} \mathcal{C}^{-1}(\tilde{\boldsymbol{\rho}} - \bar{\boldsymbol{\rho}}) - \boldsymbol{\varepsilon}(\tilde{\boldsymbol{u}} - \bar{\boldsymbol{u}}) = \mathbf{0} & \text{in} \quad \Omega, \\ -\mathbf{div}(\tilde{\boldsymbol{\rho}} - \bar{\boldsymbol{\rho}}) = \mathbf{0} & \text{in} \quad \Omega, \\ \tilde{\boldsymbol{u}} - \bar{\boldsymbol{u}} = \boldsymbol{g} - \boldsymbol{g}_h & \text{on} \quad \Gamma. \end{cases}$$

Therefore, using the continuity of the solution with respect to the corresponding data to this kind of problem (cf. (19)), we have that

$$\|(\tilde{\boldsymbol{\rho}} - \bar{\boldsymbol{\rho}}, \tilde{\boldsymbol{u}} - \bar{\boldsymbol{u}})\|_{\boldsymbol{H}} \leq \bar{C}\|\boldsymbol{g} - \boldsymbol{g}_h\|_{[H^{1/2}(\Gamma)]^n}.$$

Remark 6 *From now on, we assume $\boldsymbol{g} \in [H^1(\Gamma)]^n$. By invoking the interpolation theorem, we deduce*

$$\|\boldsymbol{g} - \boldsymbol{g}_h\|_{[H^{1/2}(\Gamma)]^n} \leq C\|\boldsymbol{g} - \boldsymbol{g}_h\|^{1/2}_{[L^2(\Gamma)]^n}\|\boldsymbol{g} - \boldsymbol{g}_h\|^{1/2}_{[H^1(\Gamma)]^n}.$$

Remark 7 *For 2D case, under the assumption $\boldsymbol{g} \in [H^1(\Gamma)]^2$, we can take $\boldsymbol{g}_h$ as the linear Lagrange interpolation of the function $\boldsymbol{g}$, i.e., we have $\boldsymbol{g}_h(\boldsymbol{x}) = \boldsymbol{g}(\boldsymbol{x})$ for each node $\boldsymbol{x} \in \Gamma$ and $\boldsymbol{g}_h|_e \in [\mathcal{P}_1(e)]^2$ for all $e \in E(\Gamma)$, where $E(\Gamma)$ denotes de set of all edges induced by the triangulation $\mathcal{T}_h$, lying on the*

boundary Γ. *The fact that now the function* $\boldsymbol{g}-\boldsymbol{g}_h$ *vanishes at the nodes of* $\mathcal{T}_h$ *lying on* Γ, *allows us to estimate its* $[H^{1/2}(\Gamma)]^2$*-norm in terms of* L^2*-local norms on the edges of* Γ. *More precisely, according to Theorem 1 in [10], there holds*

$$\|\boldsymbol{g}-\boldsymbol{g}_h\|^2_{[H^{1/2}(\Gamma)]^2} \leq C \left\{ \log[1+C_h(\Gamma)] \sum_{j=1}^{m} h_j \left\| \frac{\partial \boldsymbol{g}}{\partial \boldsymbol{t}} - \frac{\partial \boldsymbol{g}_h}{\partial \boldsymbol{t}} \right\|^2_{[L^2(\Gamma_j)]^2} \right\},$$

where $h_j = |\Gamma_j|$, $j=1,\ldots,m$, $C_h(\Gamma) := \max\left\{\frac{h_i}{h_j} : \Gamma_i \text{ is a neighbor of } \Gamma_j,\ i,j\in\{1,...,m\}\right\}$, *and* $\{\Gamma_1,\ldots,\Gamma_m\}$ *is the partition of* Γ *induced by* $\mathcal{T}_h$. *We remind that given an edge* e *induced by* $\mathcal{T}_h$, *and lying on* Γ, *we set* $\boldsymbol{t}$ *as the tangential vector associated to* e. *In addition,* $\frac{\partial \boldsymbol{g}}{\partial \boldsymbol{t}}$ *represents the tangential derivative of* $\boldsymbol{g}$ *along* e. *Similar meaning is given to* $\frac{\partial \boldsymbol{g}_h}{\partial \boldsymbol{t}}$.

Moreover, assuming a little more regularity, that is $\boldsymbol{g}| \in [H^2(\Gamma_i)]^2$ *for* $i=1,\ldots,m$, *and taking into account Proposition 1.2 in [14], it is possible to establish that this error behaves at least as* $\mathcal{O}(h^{3/2})$, *i.e., it can be seen as a higher order term.*

Remark 8 *For the 3D case, and assuming that* $\boldsymbol{g}\in[H^1(\Gamma)]^3$, *the Sobolev interpolation theorem implies*

$$\|\boldsymbol{g}-\boldsymbol{g}_h\|^2_{[H^{1/2}(\Gamma)]^3} \leq C\|\boldsymbol{g}-\boldsymbol{g}_h\|_{[L^2(\Gamma)]^3}\|\boldsymbol{g}-\boldsymbol{g}_h\|_{[H^1(\Gamma)]^3}, \tag{25}$$

which allows us to deduce

$$\|\boldsymbol{g}-\boldsymbol{g}_h\|^2_{[H^{1/2}(\Gamma)]^3} \leq C_{\mathtt{D}} \left\{ \sum_{F\in E(\Gamma)} h_{\mathtt{D}}^2 \|\boldsymbol{g}-\boldsymbol{g}_h\|_{[H^1(F)]^3} \right\}, \tag{26}$$

where $h_{\mathtt{D}} := \max\{h_F : F\in E(\Gamma)\}$.

Furthermore, under the assumption that $\boldsymbol{u}\in H^{1+s}(\Omega)$, *with* $s>1/2$, *we have that* $g\in H^{1+\delta}(\Gamma)$, *with* $\delta>0$ *and therefore it is possible to use Lagrange interpolation. Following the same spirit of the Remark 7, we can assume a little more regularity, that is* $g\in H^2(F)$, *for each* $F\in E(\Gamma)$, *and then, after invoking Proposition 3.1 in [14], it is possible to establish that this error behaves at least as* $\mathcal{O}(h^{3/2})$, *i.e., it can be seen as a higher order term.*

4.2 A posteriori error analysis

Straightforward modifications of the analysis described in Section 3, allow us to endow the problem (24) with an a posteriori error estimator. Let $(\bar{\boldsymbol{\rho}},\boldsymbol{u})\in\boldsymbol{H}_0$ and $(\bar{\boldsymbol{\rho}}_h,\boldsymbol{u}_h)\in\boldsymbol{H}_{0,h}$ be the unique solutions of the problems (23) and (24), respectively. We define the residual

$$\tilde{R}_h(\boldsymbol{\tau},\boldsymbol{v}) := \bar{F}(\boldsymbol{\tau},\boldsymbol{v}) - A((\bar{\boldsymbol{\rho}}_h,\boldsymbol{u}_h),(\boldsymbol{\tau},\boldsymbol{v})), \qquad \forall\,(\boldsymbol{\tau},\boldsymbol{v})\in\boldsymbol{H}_0. \tag{27}$$

Taking $(\boldsymbol{\tau},\boldsymbol{v}) := (\bar{\boldsymbol{\rho}}-\bar{\boldsymbol{\rho}}_h,\boldsymbol{u}-\boldsymbol{u}_h)\in\boldsymbol{H}_0$, and after invoking the ellipticity of the bilinear form A on $\boldsymbol{H}_0$, as well as the definition of the residual (27), we deduce that

$$\|(\bar{\boldsymbol{\rho}}-\bar{\boldsymbol{\rho}}_h,\boldsymbol{u}-\boldsymbol{u}_h)\|_{\boldsymbol{H}} \leq C^{-1}_{\mathtt{ell}} \sup_{\substack{(\boldsymbol{\tau},\boldsymbol{v})\in\boldsymbol{H}_0\\(\boldsymbol{\tau},\boldsymbol{v})\neq(0,0)}} \frac{\tilde{R}_h((\boldsymbol{\tau},\boldsymbol{v}))}{\|(\boldsymbol{\tau},\boldsymbol{v})\|_{\boldsymbol{H}}}. \tag{28}$$

In the next lemma, we collect an upper bound for the residual

ν	μ	λ
0.4900	0.3356	16.4430
0.4999	0.3334	1666.4444

Table 1: Lamé parameters, for some values of Poisson ratio ν

Lemma 9 *There exists a positive constant C, independent of h, such that*

$$\sup_{\substack{(\boldsymbol{\tau},\boldsymbol{v})\in \boldsymbol{H}_0 \\ (\boldsymbol{\tau},\boldsymbol{v})\neq(0,0)}} \frac{\tilde{R}_h(\boldsymbol{\tau},\boldsymbol{v})}{\|(\boldsymbol{\tau},\boldsymbol{v})\|_{\boldsymbol{H}}} \leq C \left(||\boldsymbol{f} + \mathbf{div}(\bar{\boldsymbol{\rho}}_h)||_{[L^2(\Omega)]^n} + ||\boldsymbol{\varepsilon}(\boldsymbol{u}_h + \boldsymbol{w}_h) - \mathcal{C}^{-1}\bar{\boldsymbol{\rho}}_h||_{[L^2(\Omega)]^{n\times n}} \right).$$

Proof. Taking into account the definitions of the linear functional $\bar{F}$ as well as of the bilinear form A, the proof follows the same ideas than the ones described in Section 3. We omit further details. □

Then, we define the a posteriori error estimator η as follows:

$$\eta^2 := \sum_{T\in\mathcal{T}_h} \eta_T^2, \quad \text{with} \quad \eta_T^2 := \|\boldsymbol{f} + \mathbf{div}(\bar{\boldsymbol{\rho}}_h)\|^2_{[L^2(T)]^n} + \|\boldsymbol{\varepsilon}(\boldsymbol{u}_h + \boldsymbol{w}_h) - \mathcal{C}^{-1}\bar{\boldsymbol{\rho}}_h\|^2_{[L^2(T)]^{n\times n}}, \tag{29}$$

for each $T \in \mathcal{T}_h$.

The reliability and the local efficiency of η, are established in the next result.

Theorem 10 *Let $(\bar{\boldsymbol{\rho}}, \boldsymbol{u}) \in \boldsymbol{H}_0$ and $(\bar{\boldsymbol{\rho}}_h, \boldsymbol{u}_h) \in \boldsymbol{H}_{0,h}$ be the unique solutions to problems* (23) *and* (24)*, respectively. Then, there exists a positive constant $C_{\mathtt{rel}}$, independent of h, such that*

$$\|(\bar{\boldsymbol{\rho}} - \bar{\boldsymbol{\rho}}_h, \boldsymbol{u} - \boldsymbol{u}_h)\|_{\boldsymbol{H}} \leq C_{\mathtt{rel}}\, \eta, \tag{30}$$

and there exists a positive constant $C_{\mathtt{eff}}$, independent of h and T, such that

$$C_{\mathtt{eff}}\, \eta_T \leq \|(\bar{\boldsymbol{\rho}} - \bar{\boldsymbol{\rho}}_h, \boldsymbol{u} - \boldsymbol{u}_h)\|_{H(\mathbf{div},T)\times[H^1(T)]^n}, \qquad \forall\, T \in \mathcal{T}_h. \tag{31}$$

Proof. The proof is analogous to the proof of Theorem 3. We omit further details. □

5 Numerical experiments

In this section we present several numerical results that illustrate the performance of the augmented scheme (24) and the a posteriori error estimator η for the simplest finite element subspace $\boldsymbol{H}_{0,h}$ defined in Section 4.

We recall that given the Young modulus E and the Poisson ratio ν of a linear elastic material, the corresponding Lamé parameters are defined by $\mu := \frac{E}{2(1+\nu)}$ and $\lambda := \frac{E\,\nu}{(1+\nu)\,(1-2\,\nu)}$. In the examples below, we take $E = 1$ and consider the values $\nu = 0.4900$ and $\nu = 0.4999$, which yield the following values of μ and λ that are shown in Table 1. The adaptive refinement algorithm we consider can be found in [16], and reads as follows:

EXAMPLE	Ω	ν	$u_1(x_1,x_2) = u_2(x_1,x_2)$
1	$(0,1)^2$	0.4900 0.4999	$\dfrac{x_1\,(x_1-1)\,x_2\,(x_2-1)}{(x_1-1)^2+(x_2-1)^2+0.01}$
2	$(0,1)^2$	0.4900	$x_1\,x_2\,\mathrm{e}^{x_1+x_2}$
3	$(-0.25,0.25)^2 \setminus [0,0.25]^2$	0.4900	$\dfrac{x_1\,x_2}{(x_1^2+x_2^2)^{1/3}} + 2x_2$
4	$(0,1)^2 \setminus \{\boldsymbol{x}\in\mathbb{R}^2 : \|\boldsymbol{x}\| \le 0.1\}$	0.4900	$\dfrac{10^{-4}}{x_1^2+x_2^2-0.05^2}$

Table 2: Domain Ω, values of ν and exact solution $\boldsymbol{u} = (u_1,u_2)^{\mathtt{t}}$ for the first 4 examples

Algorithm 1: Adaptive Refinement Algorithm

Result: Improvement of quality of approximation
Input: tolerance `tol`, initial / coarse mesh $\mathcal{T}_h^0$;
`Step 1:` Solve the Galerkin scheme for the current mesh $\mathcal{T}_h^0$. Then compute $\{\eta_T\}_{T\in\mathcal{T}_h^0}$.
while $\eta >$ `tol` **do**
  `Mark each element` $T'\in\mathcal{T}_h$ `such that`

$$\eta_{T'} \ge \frac{1}{2}\max\{\eta_T : T\in\mathcal{T}_h\}.$$

  `Refine marked elements and remove hanging nodes if corresponds;`
  `This generates an adapted mesh` $\mathcal{T}_h$;
  $\mathcal{T}_h^0 \leftarrow \mathcal{T}_h$ `and go to Step 1.`
end

In Table 2 below, we specify the four examples to be considered in this section. By simplicity, all examples are in 2D. We choose the data $\boldsymbol{f}$ and $\boldsymbol{g}$ so that the exact solution is $\boldsymbol{u}(x_1,x_2) := (u_1(x_1,x_2),u_2(x_1,x_2))^{\mathtt{t}}$.

We first emphasize the robustness of the approach and the a posteriori error estimator η with respect to the Poisson ratio. We approximate the solution of Example 1 for two different values of ν using a sequence of uniform / adapted meshes. Hereafter, uniform refinement means that given a uniform initial triangulation, each subsequent mesh is obtained from the previous one by dividing each triangle into the four ones arising when connecting the midpoints of its sides. In Figure 1 and Figure 2 we present the total errors vs degrees of freedom (cf. Figures (1a) and (2a)), and the efficiency indices (cf. Figures (1b) and (2b)) obtained for Example 1 with $\nu = 0.4900$ and $\nu = 0.4999$, respectively. In both cases we can see that the scheme converges with the optimal convergence rate and the efficiency indices remain constant, close to 1. This shows that both, the scheme and the estimator, remain locking free.

In what follows, we take $\nu = 0.4900$ and consider Examples 2, 3 and 4 to illustrate the performance of the adaptive Algorithms 1, based on η. We use Example 2 to illustrate the behavior of the scheme and the estimator when we deal with no null boundary term. We observe, in Figure 3, the robustness

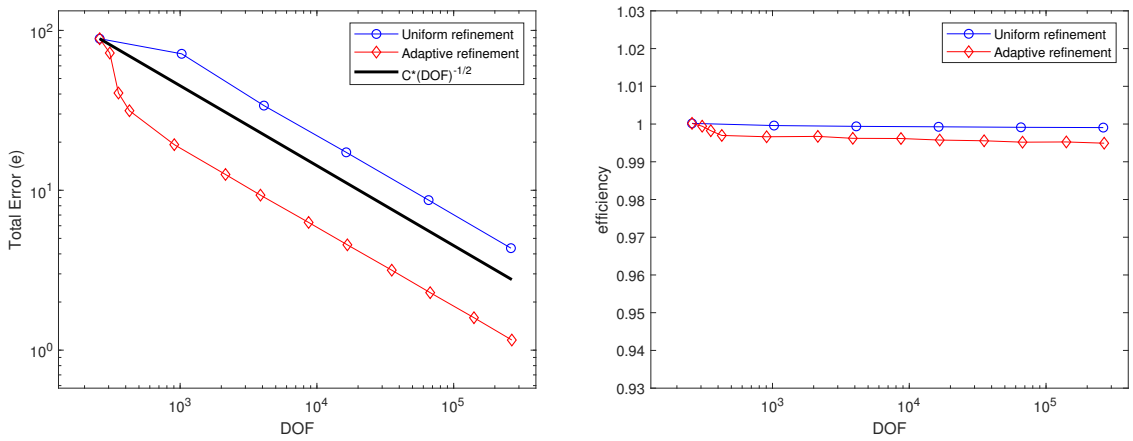

(a) (b)

Figure 1: (a) Total errors vs. DOFs for Example 1, with Poisson ratio $\nu = 0.49$, using uniform and adaptive refinements. (b) Corresponding efficiency indices vs. DOFs on both kind of refinements.

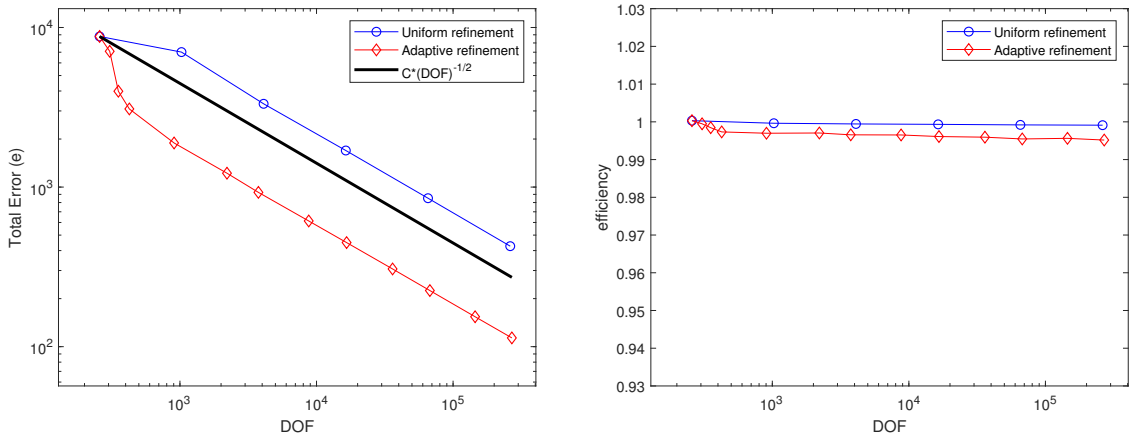

(a) (b)

Figure 2: (a) Total errors vs. DOFs for Example 1, with Poisson ratio $\nu = 0.4999$, using uniform and adaptive refinements. (b) Corresponding efficiency indices vs. DOFs on both kind of refinements.

of the scheme and the estimator when working with non-homogeneous boundary data. Its convergence rate is optimal and the efficiency index remains lower and upper bound.

We remark that the solution of Example 3 has a singularity at the boundary point $(0, 0)$. In fact, the behavior of $\boldsymbol{u}$ in a neighborhood of the origin implies that $\mathbf{div}(\boldsymbol{\sigma}) \in [H^{1/3}(\Omega)]^2$. Thus, the expected rate of convergence for the uniform refinement is $1/3$. On the other hand, the solution of Example 4 shows large stress regions around the curve $x_1^2 + x_2^2 = 0.05^2$. In Figures 4 and 6 we observe that the errors in the adaptive procedures decrease much faster than in the uniform one. In particular, we can observe in Figure 4a that, for Example 3, the experimental convergence rates for the uniform refinement procedure approach $1/3$, as predicted by the theory. Furthermore, we see that the adaptive

Algorithm 1, based on η, is able to recover the linear convergence. We also observe that the efficiency indices in Example 3 are always in a neighborhood of 1.0, which confirms the reliability and eventual efficiency of the a posteriori error estimator η. Some adapted meshes are reported in Figure 5, where we can see that the a posteriori error estimator recognizes the singularity.

For Example 4, the convergence of the adaptive Algorithm 1, based on η, is faster than the corresponding to the uniform refinement procedure, as can be seen from Figure 6a. In Figure 6b, we display the efficiency indices of η, and we observe that, again, it is close to 1. This confirms the reliability and eventual efficiency of the a posteriori error estimator. In addition, Figure 7 shows the ability of Algorithm 1, to recognize the region where the greatest stresses are concentrated.

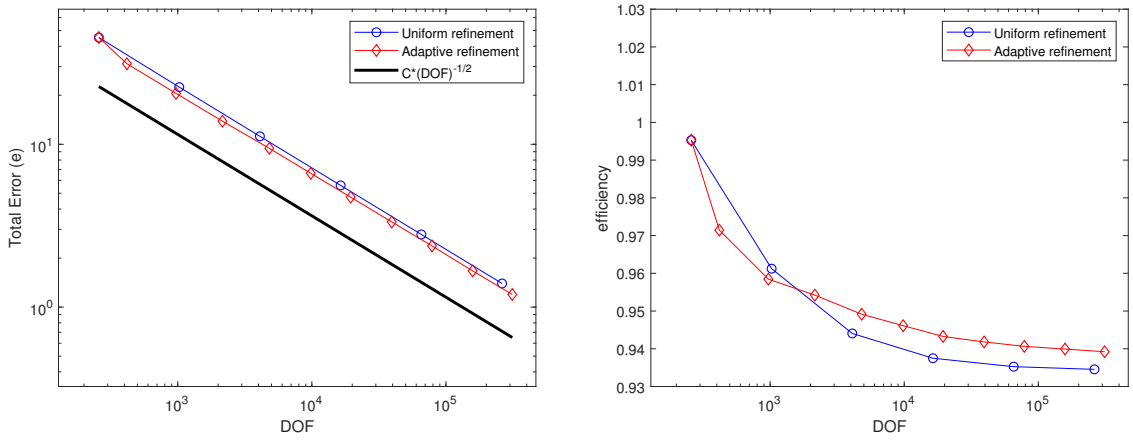

(a) (b)

Figure 3: (a) Total errors vs. DOFs for Example 2, with Poisson ratio $\nu = 0.49$, using uniform and adaptive refinements. (b) Corresponding efficiency indices vs. DOFs on both kind of refinements.

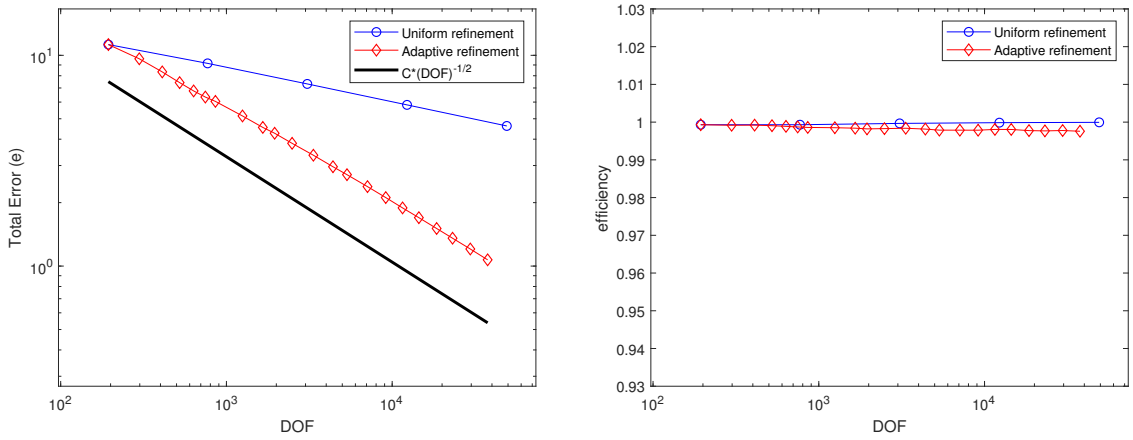

(a) (b)

Figure 4: (a) Total errors vs. DOFs for Example 3, with Poisson ratio $\nu = 0.49$, using uniform and adaptive refinements. (b) Corresponding efficiency indices vs. DOFs on both kind of refinements.

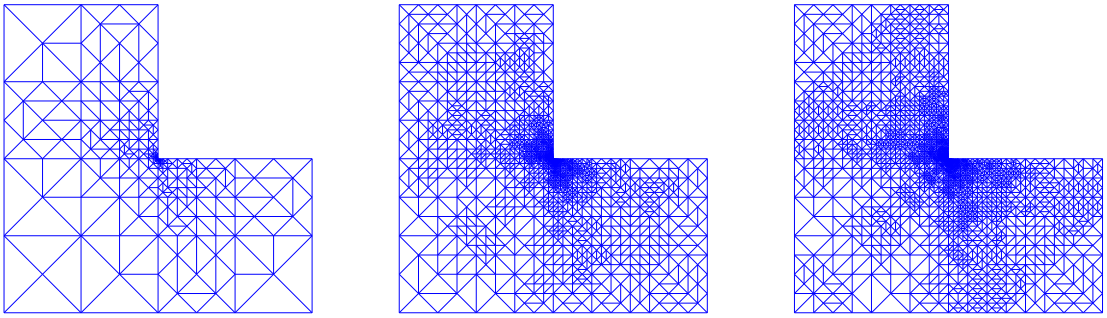

(a) (b) (c)

Figure 5: Some adapted meshes for Example 3, obtained with Algorithm 1, corresponding to (a) 1954, (b) 14490 and (c) 23138 DOFs, respectively.

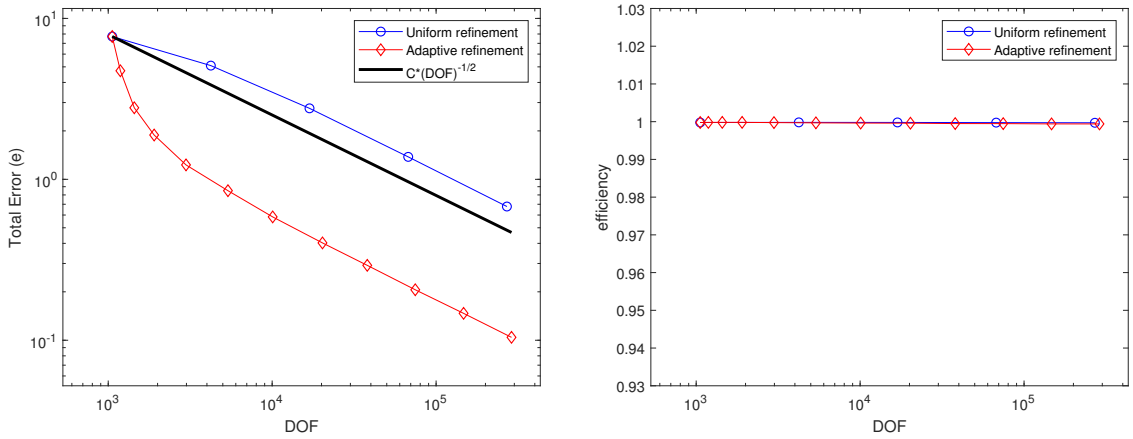

(a) (b)

Figure 6: (a) Total errors vs. DOFs for Example 4, with Poisson ratio $\nu = 0.49$, using uniform and adaptive refinements. (b) Corresponding efficiency indices vs. DOFs on both kind of refinements.

5.1 Another singular test

Here we consider an example described in [11] (see Section 7.6.4.2, page 371), where the components of the displacement are different from each other and its gradient has a singularity at origin. In order to introduce it, we introduce $A := \{(x_1, x_2) \in \mathbb{R}^2 \ : \ \ |x_1 + \frac{\sqrt{2}}{2}| + |x_2| \leq \frac{\sqrt{2}}{2}\}$, and we define the L-shape domain $\Omega := \{(x_1, x_2) \in \mathbb{R}^2 \ : \ \ |x_1| + |x_2| < \sqrt{2}\} \setminus A$. The displacement of the solution, in polar coordinates (r, θ), is given by

$$\boldsymbol{u}(r,\theta) = \frac{1}{2G} r^L \begin{pmatrix} (\kappa - Q(L+1))\cos(L\theta) - L\cos((L-2)\theta) \\ (\kappa + Q(L+1))\sin(L\theta) + L\sin((L-2)\theta) \end{pmatrix},$$

where the various parameters take the following numerical values: $E = 1$, $\nu = 3$, $G = \frac{5}{13}$, $\kappa = \frac{9}{5}$, $L = 0,5444837367825$, $Q = 0,5430755788367$. The forcing term in this case is equal to zero, while the Dirichlet boundary condition is inferred from the exact solution. In Figure 8 we display the rate

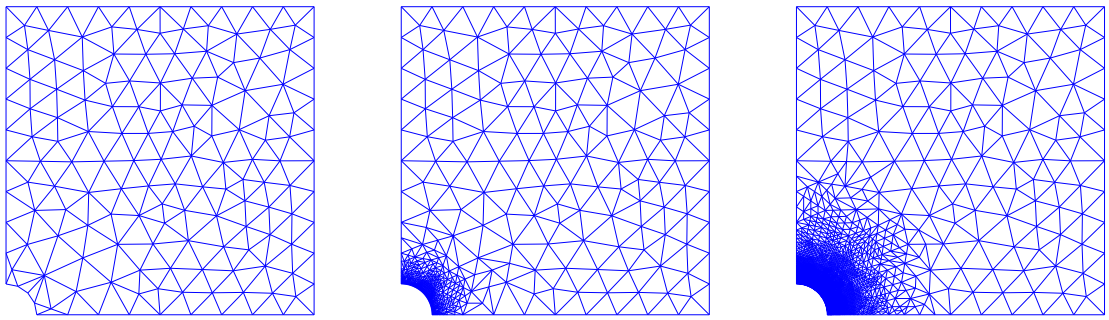

(a) (b) (c)

Figure 7: Example 4: Initial and adapted meshes, generated after applying Algorithm 1, corresponding to (a) 1058, (b) 5374 and (c) 74610 DOFs, respectively.

convergence (cf. Figure 8a) and efficiency indices of η (cf. Figure 8b). We see that the adaptive scheme is capable of converging linearly as if the solution were smooth, while the uniform refinement converges with L-rate. Furthermore, the efficiency indexes remain bound. The ability to detect the singularity is exhibited in Figure 9, which confirms that the estimator is indeed detecting the place where it is.

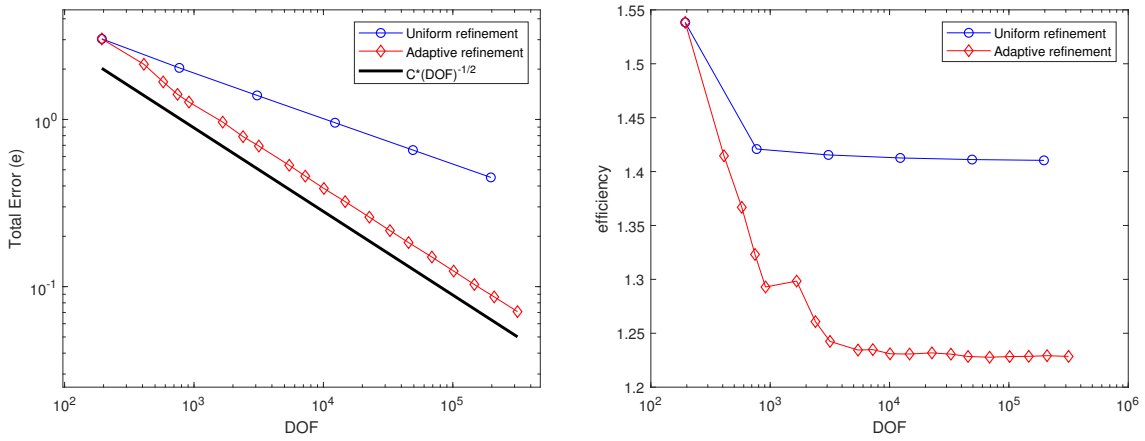

(a) (b)

Figure 8: (a) Total errors vs. DOFs for Example 5, with Poisson ratio $\nu = 3$, using uniform and adaptive refinements. (b) Corresponding efficiency indices vs. DOFs on both kind of refinements.

Concluding remarks

In this paper, we develop a reliable and local efficient a posteriori error estimator for linear elasticity problem with non homogeneous displacement on the boundary. We deal with a locking-free augmented variational formulation, which is well posed and does not include a penalization term of the Dirichlet condition. To circumvent that, we first perform a homogenization technique that yields to analize a

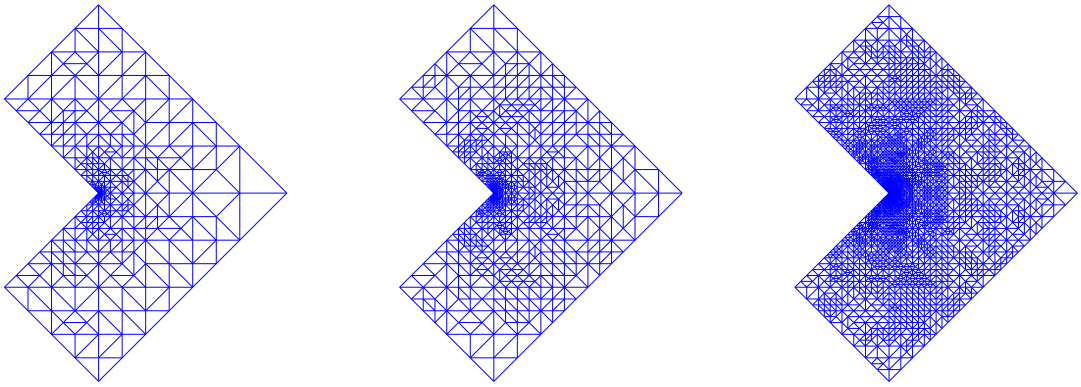

(a) (b) (c)

Figure 9: Some adapted meshes for Example 5 obtained with Algorithm 1, corresponding to (a) 1954, (b) 14490 and (c) 23138 DOFs, respectively.

variant of the linear elasticity problem, but with homogeneous displacement on the boundary. As a consequence, the resulting a posteriori error estimator consists of two element residual terms, which shows the low cost (computationally speaking) of our estimator. Numerical experiments are in agreement with the obtained theoretical results. We check the locking-free behaviour of the scheme when the Poisson ratio ν is close to $1/2$. Moreover, the proposed adapted refinement Algorithm 1 helps to detect and refine such region of the domain where the estimator is more dominant. Finally, is important to remark that the current approach, described in this work, could be extended to deal with other types of problems.

Acknowledgments

The authors have been partially supported by ANID-Chile through FONDECYT grant 1200051. Moreover, T. Barrios and E. Behrens have been partially supported by Dirección de Investigación of Universidad Católica de la Santísima Concepción (Chile), through project FGII-04/2023. All authors have contributed equally in this article.

References

[1] J. A. Almonacid, G. N. Gatica and R. Ruiz-Baier, Ultra-weak symmetry of stress for augmented mixed finite element formulations in continuum mechanics. Calcolo, 57, 1, article: 2, (2020).

[2] D.N. Arnold, F. Brezzi and J. Douglas, PEERS: A new mixed finite element method for plane elasticity. Japan Journal of Industrial and Applied Mathematics, 1, 2, 347–367, (1984).

[3] T.P. Barrios, E.M. Behrens and M. González. A posteriori error analysis of an augmented mixed formulation in linear elasticity with mixed and Dirichlet boundary conditions. Computer Methods in Applied Mechanics and Engineering, 200, 101–113, (2011).

[4] T. P. Barrios, E. M. Behrens and M. González. Low cost A posteriori error estimators for an augmented mixed FEM in linear elasticity. Applied Numerical Mathematics, 84, 46–65, (2014).

[5] T. P. Barrios, J. M. Cascón and M. González, *A posteriori error estimation of a stabilized mixed finite element method for Darcy flow*. In book: Proceedings of International conference Boundary and Interior Layers - Computational & Asymptotic Methods, BAIL 2014 (Edited by Petr Knobloch). Springer series Lecture Notes in Computational Science and Engineering, 108, 13 – 23, (2015).

[6] T.P. Barrios, G.N. Gatica, M. González and N. Heuer. A residual based a posteriori error estimator for an augmented mixed finite element method in linear elasticity. M2AN Mathematical Modelling and Numerical Analysis, 40, 5, 843–869, (2006).

[7] D. Braess. Finite Elements. Theory, Fast Solvers, and Applications in Solid Mechanics. Cambridge University Press, 1997.

[8] F. Brezzi and M. Fortin. Mixed and hybrid finite element methods. Springer Series in Computational Mathematics 15, Springer-Verlag, New York, 1991.

[9] J. Camaño, R. Oyarzúa , R. Ruiz-Baier , G. Tierra. Error analysis of an augmented mixed method for the Navier-Stokes problem with mixed boundary conditions, IMA Journal of Numerical Analysis, 38, 1452–1484, (2018).

[10] C. Carstensen. An a posteriori error estimate for a first-kind integral equation. Mathematics of Computation, 66, 139–155, (1997).

[11] D. A. Di Pietro, J. Droniou: The Hybrid High-Order Method for Polytopal Meshes: Design, Analysis, and Applications. Number 19 in Modeling, Simulation and Applications, Springer International Publishing, 2020. ISBN 978-3-030-37202-6 (Hardcover) 978-3-030-37203-3 (eBook). DOI: 10.1007/978-3-030-37203-3

[12] G.N. Gatica. Analysis of a new augmented mixed finite element method for linear elasticity allowing $\mathbb{RT}_0$-$\mathbb{P}_1$-$\mathbb{P}_0$ approximations. M2AN Mathematical Modelling and Numerical Analysis, 40, 1, 1–28, (2006).

[13] G.N. Gatica. An augmented mixed finite element method for linear elasticity with non-homogeneous Dirichlet conditions. Electronic Transactions on Numerical Analysis, 26, 421–438, (2007).

[14] M.G. Larson and F. Bengzon. The Finite Element Method: Theory, Implementation and Applications. Springer-Verlag, Berlin, Heidelberg, 2013.

[15] R. Stenberg, A family of mixed finite elements for the elasticity problem. Numerische Mathematik, 53, 513–538, (1988) .

[16] R. Verfürth, A Review of a Posteriori Error Estimation and Adaptive Mesh-Refinement Techniques, Wiley-Teubner, Chichester, 1996.

Centro de Investigación en Ingeniería Matemática (CI^{2}MA)

PRE-PUBLICACIONES 2024

2024-10 Kaïs Ammari, Vilmos Komornik, Mauricio Sepúlveda, Octavio Vera: *Stability of the Rao-Nakra sandwich beam with a dissipation of fractional derivative type: theoretical and numerical study*

2024-11 Lady Angelo, Jessika Camaño, Sergio Caucao: *A skew-symmetric-based mixed FEM for stationary MHD ows in highly porous media*

2024-12 Gabriel N. Gatica: *A note on the generalized Babuska-Brezzi theory: revisiting the proof of the associated Strang error estimates*

2024-13 Carlos D. Acosta, Raimund Bürger, Julio Careaga, Stefan Diehl, Romel Pineda, Daniel Támara: *A semi-implicit method for a degenerating convection-diffusion-reaction problem modeling secondary settling tanks*

2024-14 Gabriel N. Gatica, Cristian Inzunza, Ricardo Ruiz-Baier: *Primal-mixed finite element methods for the coupled Biot and Poisson-Nernst-Planck equations*

2024-15 Isaac Bermudez, Víctor Burgos, Jessika Camaño, Fernando Gajardo, Ricardo Oyarzúa, Manuel Solano: *Mixed finite element methods for coupled fluid flow problems arising from reverse osmosis modeling*

2024-16 Mario Álvarez, Gonzalo A. Benavides, Gabriel N. Gatica, Esteban Henriquez, Ricardo Ruiz-Baier: *Banach spaces-based mixed finite element methods for a steady sedimentation-consolidation system*

2024-17 Tomás Barrios, Edwin Behrens, Rommel Bustinza, Jose M. CASCON: *An a posteriori error estimator for an augmented variational formulation of the Brinkman problem with mixed boundary conditions and non-null source terms*

2024-18 Sergio Caucao, Gabriel N. Gatica, Luis F. Gatica: *A posteriori error analysis of a mixed finite element method for the stationary convective Brinkman–Forchheimer problem*

2024-19 Isaac Bermudez, Jessika Camaño, Ricardo Oyarzúa, Manuel Solano: *A conforming mixed finite element method for a coupled Navier–Stokes/transport system modelling reverse osmosis processes*

2024-20 Ana Alonso-Rodriguez, Jessika Camaño, Ricardo Oyarzúa: *Analysis of a FEM with exactly divergence-free magnetic field for the stationary MHD problem*

2024-21 Tomás Barrios, Edwin Behrens, Rommel Bustinza: *On the approximation of the Lamé equations considering nonhomogeneous Dirichlet boundary condition: A new approach*

Para obtener copias de las Pre-Publicaciones, escribir o llamar a: Director, Centro de Investigación en Ingeniería Matemática, Universidad de Concepción, Casilla 160-C, Concepción, Chile, Tel.: 41-2661324, o bien, visitar la página web del centro: `http://www.ci2ma.udec.cl`







Centro de Investigación en
Ingeniería Matemática (CI²MA)
Universidad de Concepción

Casilla 160-C, Concepción, Chile
Tel.: 56-41-2661324/2661554/2661316
http://www.ci2ma.udec.cl